SUPPLEMENTARY APPENDIX

SUPPLEMENTARY METHODS

Establishment of a genetically engineered mouse model of Etv6-NTRK3 B-ALL

Etv6-NTRK3 conditional knock-in mice crossed with the *Rosa-Stop-YFP* reporter were generated as previously described.[1] Briefly, the human portion of NTRK3 cDNA encoding the tyrosine kinase domain was inserted into exon 6 of the mouse *Etv6* locus, downstream of a floxed transcriptional terminator sequence. *CD19-Cre* mice (B6.129P2(C)-*Cd19*$^{tm1(cre)Cgn}$/J) were obtained from The Jackson Laboratory.[2] Genotyping was performed by polymerase chain reaction (PCR) using primers listed in supplemental Table 1. All experiments were approved by the St Jude Children's Research Hospital Institutional Animal Care and Use Committee.

Pathology and flow cytometry

For histopathological analysis, tissues were fixed in 4% neutral buffered formalin and routinely processed, embedded and stained with hematoxylin and eosin (H&E). Images were acquired using an Olympus BX41 with attached microscope camera (SPOT Insight Color Mosaic 2MP) and captured with SPOT imaging software. Immunophenotyping was performed on bone marrow for B220, CD19, CD43, BP1, IgM, CD3, Mac-1 and Gr-1 (BD Biosciences). Cells were collected on an LSR II flow cytometer (BD Biosciences) and analyzed using FlowJo (Tree Star).

Array-based comparative genomic hybridization of mouse tumors

The Mouse Genome CGH 244K microarray (G4415A; Agilent, Santa Clara, CA) was customized by replacing sex chromosome probes with over 17,000 probes interrogating the 20 gene loci (± 100kb) corresponding to the genes targeted by recurring DNA copy number alterations in human B-ALL (*Bcl11a, Cdkn2a, Ebf1, Ikzf1, Ikzf2, Ikzf3, Il7r, Lef1, Mdm2, Mef2c, Myb, Pax5, Pten, Rb1, Sfpi1, Sox4, Stat5a, Tcf3, Tcf4* and *Trp53*).[3, 4] Median probe spacing was 250 bp. Array hybridization was performed according to the manufacturer's recommended protocols. In brief, tumor and non-tumor (B220+ splenocytes) genomic DNA was labeled using

the Agilent ULS Labeling kit. Hybridization was carried out in an Agilent oven at 65°C for 40 hours at 20 rpm followed by standard wash procedures. The microarray was then scanned in an Agilent scanner at 3μm resolution, and the array data was extracted using the default CGH settings with Lowess dye bias correction normalization of Agilent Feature Extraction Software. The circular binary segmentation algorithm implemented in the DNAcopy package from Bioconductor was then applied to the normalized log2 ratio data to identify copy number alterations (CNA) for each tumor sample. We used the following cutoffs to obtain potential CNAs: (1) abs(seg.mean) >= 0.2; (2) >= 3 markers per segment. CNAs sharing same boundaries present in multiple samples were considered likely inherited copy number variants (CNV) or technical artifacts and were not included in downstream analyses.

RNA-sequencing analysis

Transcriptome analysis was performed using the Truseq total-stranded library preparation on the Illumina HiSeq 2000 platform. Fastq sequences derived from total RNA paired-end 100 bp sequences were mapped to the hg19 genome with the STRONGARM pipeline which employs bwa[5] and STAR aligner.[6] Transcript level data was counted using HTSEQ (Anders et. al, 2014).[7] Raw counts were voom normalized and contrasted using the empirical Bayes pipeline limma in R 3.2.3.[8] The volcano plot was visualized with STATA/MP 14.2 (College Station, TX).

Retroviral constructs and cell culture

Full length chimeric gene fusions were amplified from leukemic cell cDNA, cloned into the pCR Blunt II TOPO vector (Invitrogen), and sub-cloned into the mouse stem cell virus-internal ribosome entry site-green fluorescent protein (MSCV-ires-GFP, MIG) retroviral vector. Replication-incompetent, ecotropic retroviral particles were produced by transient transfection of 293T cells with a triple plasmid system (pMD.old.gag.pol and pCAG4-Eco) and used to infect mouse hematopoietic progenitor Ba/F3 cells. Each fusion was confirmed by reverse-transcription followed by PCR (RT-PCR). Cells were grown in RPMI supplemented with 10%

fetal calf serum (FCS; Sigma), 10 mmol/L L-glutamine, 1% penicillin/streptomycin/glutamine (Gibco) and 10 ng/ml IL-3 for Ba/F3 cells expressing MIG empty vector. Ba/F3 cells transduced with retroviral constructs expressing kinase fusions were cultured in the absence of cytokine.

Tyrosine kinase inhibitor screening

Ba/F3 cells were plated at 20,000 cells/well in triplicate in 96-well plates in increasing concentrations of drug. After 48 hours of incubation, drug sensitivity was determined using the CellTiter-Blue Cell Viability Assay (Promega) according to manufacturer's instructions. Compound activity for each cell line was normalized to 100% using the DMSO only as a negative control. IC_{50} values were determined using nonlinear regression (GraphPad Prism v6.0). The activity of crizotinib and larotrectinib was assessed against a panel of 79 human cancer cell lines selected from the OncoPanel collection (supplemental Table 2). Cell lines were seeded into 384-well plates in RPMI 1640 medium supplemented with 10% FCS, 2 mmol/L L-glutamine and 1 mmol/L sodium pyruvate. Compounds were added the day following cell seeding. After 72 incubation, cells were fixed and stained with nuclear dye to allow imaging of nuclei. Automated fluorescence microscopy was carried out using a Molecular Devices ImageXpress Micro XL high-content imager and images were analyzed with MetaXpress 5.1.0.41 software.

Pre-clinical treatment studies

A patient-derived xenograft (PDX) model of human ETV6-NTRK3 ALL (PASBSK) was established using bone marrow from a patient treated on a Children's Oncology Group (COG) protocol.[9, 10] The patient was a 16 year old male with Ph-like ALL and near-tetraploidy (93,XXYY,-3,+5,+5,+8,+8,-9,-15,-18,+21,-22 [17]/46,XY[3]). Based on genomic profiling including SNP array analysis and transcriptome sequencing no other alterations characteristic of Ph-like ALL, such as alteration of lymphoid transcription factor genes (*IKZF1*, *PAX5*, *EBF1*) or deletion of the *CDKN2A/B* genes, were identified.[10] Primary leukemia cells (10^6 cells per

mouse) were transplanted via tail vein injection into sublethally irradiated (2.5 Gy) NOD.Cg-*Prkdc*^{scid} *Il2rg*^{tm1Wjl}/SzJ (NOD-SCID gamma-null, or NSG) mice. Bone marrow harvested from engrafted mice was transduced with lentivirus expressing YFP and luciferase to enable bioluminescent imaging of in vivo tumor burden using a Xenogen IVIS-200 system and Living Image software (Caliper Life Sciences), as previously described.[11] Engraftment was monitored weekly by luciferase imaging. For efficacy studies, mice were randomized to receive vehicle or treatment when leukemia burden reached 10^8 photons/second. PLX7486 was provided as chow (Plexxikon) for 12 weeks. Larotrectinib (Loxo Oncology) was administered by oral gavage once daily at 200mg/kg/day in Labrafac (Gattefossé) for 6 weeks. For combination studies, dexamethasone sodium phosphate injection solution was administered at 4mg/L in drinking water. A sulfamethoxazole (600 mg/L) / trimethoprim (120 mg/L) oral suspension was added 3 days per week, and 1000 mg/L of tetracycline (Sigma) was administered daily. Blood was collected for pharmacokinetic studies at 1, 4 and 24 hours. Spleen and bone marrow were harvested at time of sacrifice and assessed for human CD45$^+$/human CD19$^+$ blasts. The mean percentage of human CD45$^+$/CD19$^+$ cells in the peripheral blood, bone marrow and spleen and splenic weight of vehicle- and inhibitor-treated animals for each PDX model were calculated at the indicated time points and compared using the unpaired student t-test.

Phosphoflow analysis

To assess in vivo phosphorylation, NSG mice engrafted with PDX PASBSK cells were treated with a single dose of vehicle, larotrectinib (200mg/kg p.o.) or PLX7486 (30mg/kg p.o). Bone marrow was harvested after 2, 8 and 24 hours. Cells were adjusted to 1 x 10^6 cells/ml and fixed, permeabilized and stained with human CD45-BV605 and human CD19-PE and either anti-STAT5 (pY694)-Ax647, anti-ERK1/2 (T202/Y204)-Ax647 (BD Biosciences), anti-STAT3 (pY705) or anti-S6 (S235/S236) (Cell Signaling Technology) followed by anti-rabbit BV421 conjugated to

anti-mouse IgG secondary antibody for pSTAT3 and pS6 (Life Technologies). Cells were collected on an LSR II flow cytometer (BD Biosciences) and analyzed using FlowJo (Tree Star).

Supplementary Table 1. Primers for genotyping *Etv6-NTRK3/+*;*CD19-Cre* mice

Primer name	5' to 3'	Comments
5POLY(A)1	ctgaggcggaaagaaccagctg	Detection of Etv6-NTRK3 and wild-type ETV6
5TEL16356	agcaggagagaccacttcccagc	Detection of Etv6-NTRK3 and wild-type ETV6
3TEL16677	tggtcatgaattgtttactgaggtccta	Detection of Etv6-NTRK3 and wild-type ETV6
3NEO43	accgcattaaagcttggctggac	Single band when positive
3STOPPER2	tggcaagtggtattccgtaagaac	Single band when positive
R26YFP-1	aaagtcgctctgagttgttat	Rosa-YFP locus
R26YFP-2	gcgaagagtttgtcctcaacc	Rosa-YFP locus
R26YFP-3	ggagcgggagaaatggatatg	Rosa-YFP locus

Supplementary Table 2. Seventy nine human cell lines screened for sensitivity to crizotinib and larotrectinib
Provided as an excel table in "Supplementary Tables".

Supplementary Table 3. Immunophenotyping and histopathological analysis for *Etv6-NTRK3/+; CD19-Cre* mice
Provided as an excel table in "Supplementary Tables".

Supplementary Table 4. aCGH analysis of *Etv6-NTRK3/+; CD19-Cre* mice
Provided as an excel table in "Supplementary Tables".

Supplementary Table 5. RNA-sequencing and limma analysis of *Etv6-NTRK3/+; CD19-Cre* mice
Provided as an excel table in "Supplementary Tables".

Supplementary Figure 1.

(A) WBC for *Etv6-NTRK3*/+; *CD19-Cre* mice compared to Etv6-NTRK3 controls. (B) RT-PCR validation of *Etv6-NTRK3* fusion in the bone marrow of *Etv6-NTRK3/+*;*CD19-Cre* mice. A faint band is observed in mouse 857, which had low YFP+ cells in the bone marrow (27%). (C) Gating strategy for immunophenotyping of bone marrow harvested from *Etv6-NTRK3*/+; *CD19-Cre* mice. Percentage of YFP+ cells in the bone marrow Error bars represent mean ± SD.

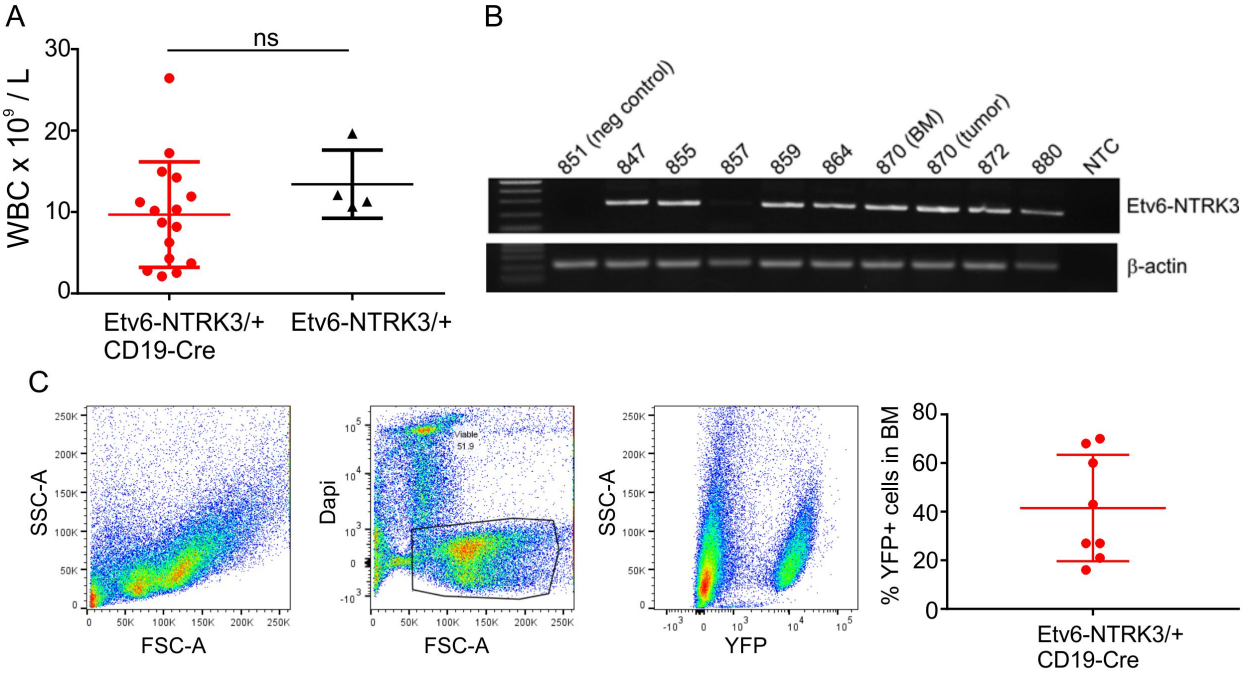

Supplementary Figure 2.

In vitro recombinant kinome screen for PLX7486 and larotrectinib. Modified from:

http://www.ecmcnetwork.org.uk/sites/default/files/PLX7486%20Background%20for%20CRUK%20Combinations%20Alliance%20%28Non-CI%29%202015-10-08%20final.pdf

https://ir.loxooncology.com/docs/events/Hyman_Larotrectinib_ASCO_2017_FINAL.PDF

PLX7486

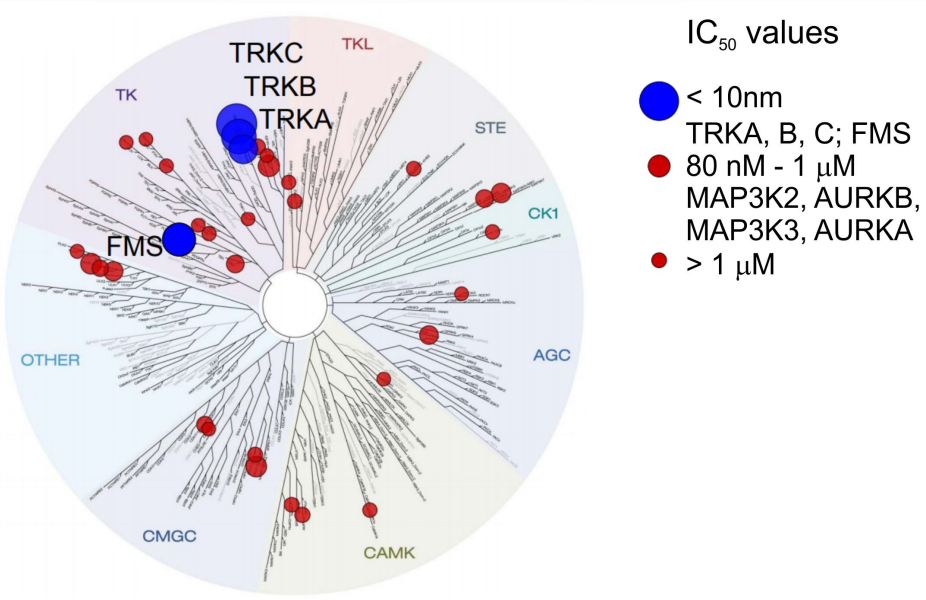

Larotrectinib

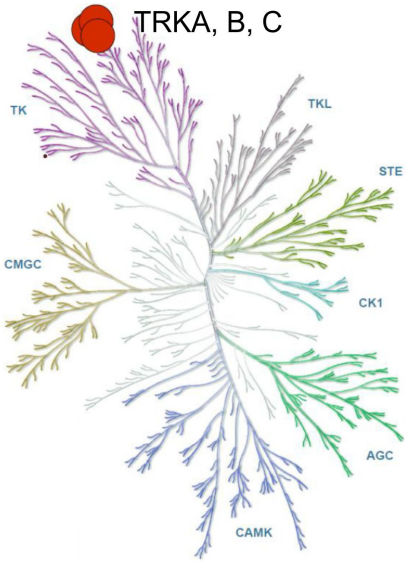

Supplementary Figure 3.

Pharmacokinetic (PK) properties of larotrectinib. One dose (200mg/kg) was administered by oral gavage and samples taken at 1, 4 and 24 hours. No difference in PK was observed with the addition of dexamethasone.

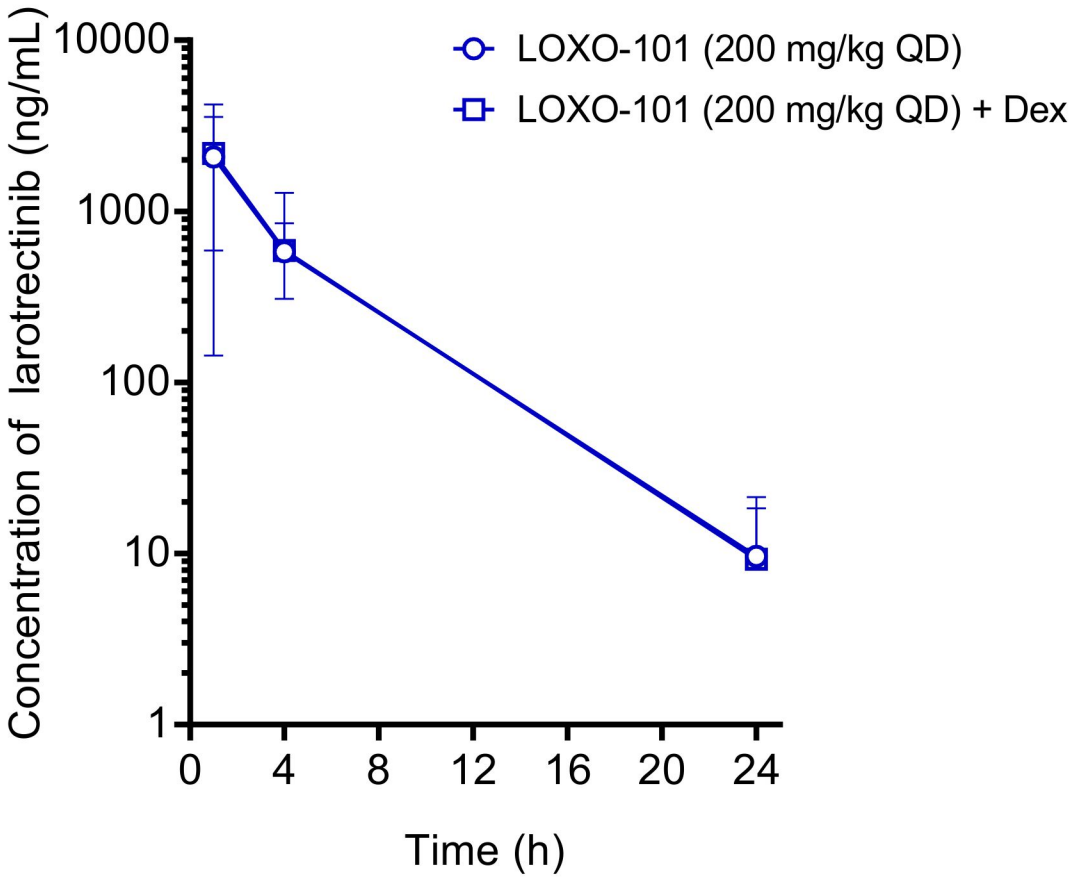

Supplementary Figure 4.

(A) The presence of human CD45^{+}/CD19^{+} leukemic blasts in the bone marrow, spleen and peripheral blood was measured by flow cytometry. Error bars represent mean ± SD. (B) Representative flow cytometry plots for infiltration of hCD45^{+}/CD19^{+} leukemic blasts in the bone marrow of vehicle, and larotrectinib-treated mice.

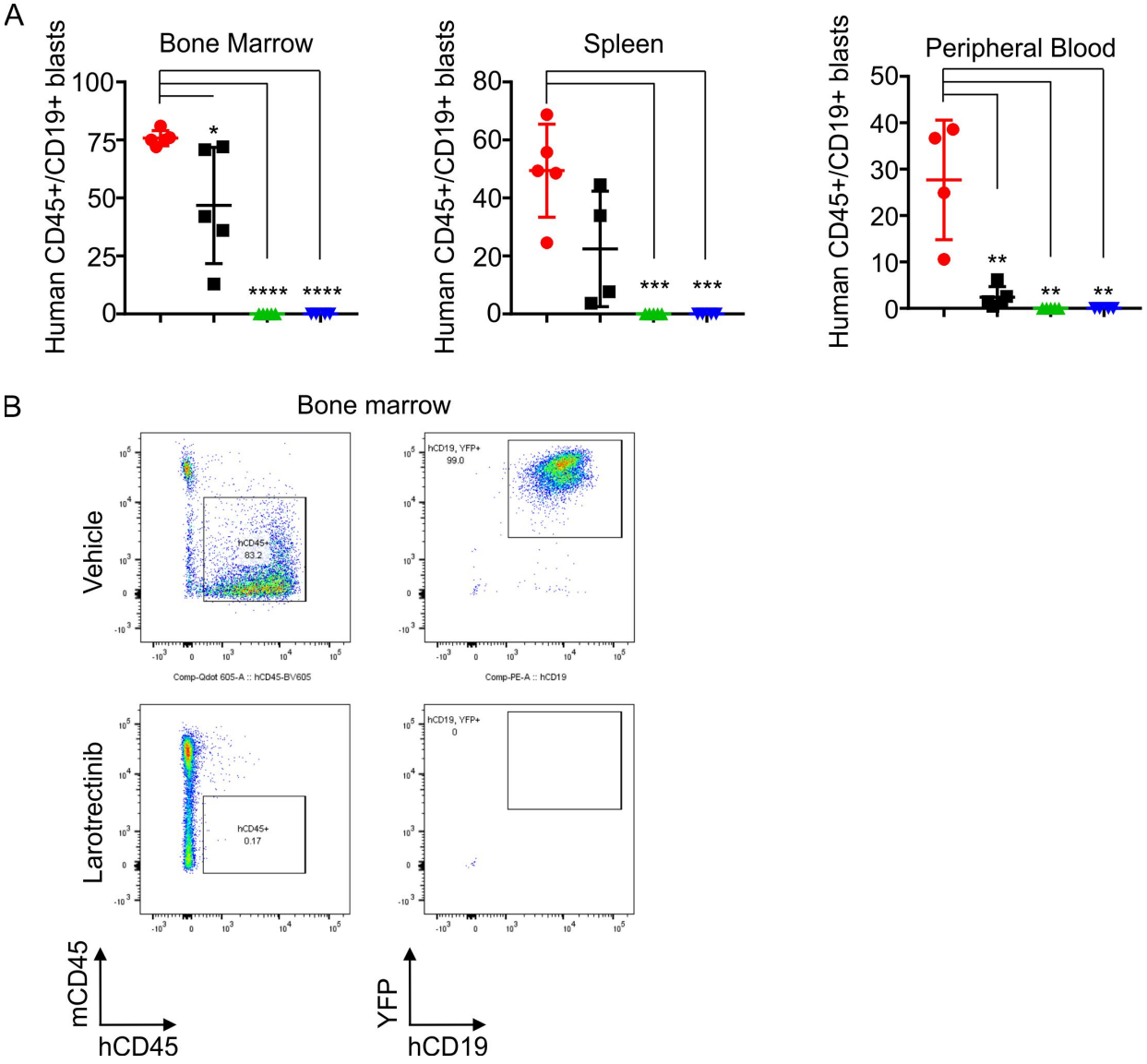

Supplementary Figure 5.

Mice engrafted with PASBSK PDX cells were treated with a single dose of vehicle, larotrectinib (200mg/kg) or PLX7486 (30mg/kg). Bone marrow was harvested at 2, 4 and 24 hours and assayed for phosphorylation of pERK1/2, pSTAT3, pSTAT5 and pS6.

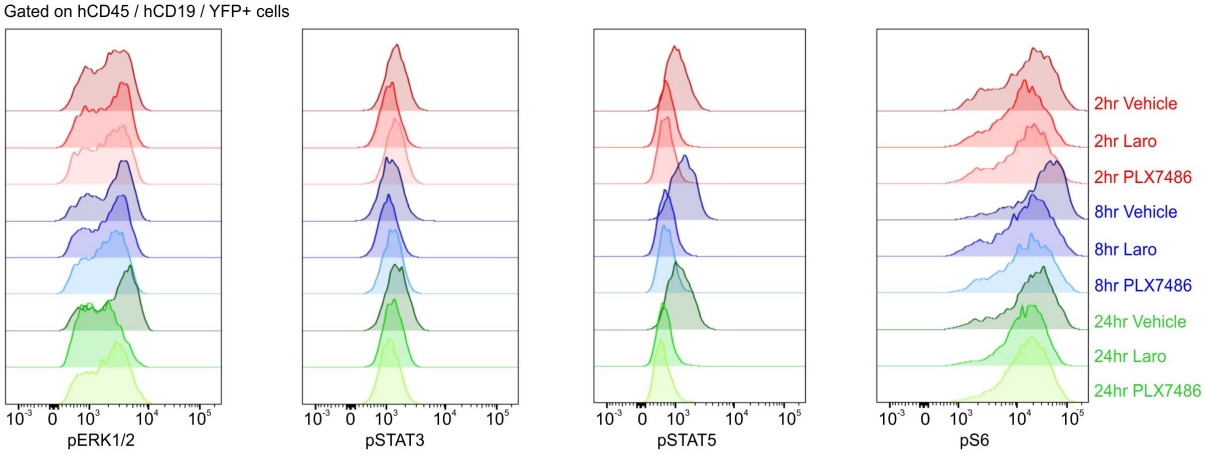

References

1. Z. Li, C. E. Tognon, F. J. Godinho, et al.: ETV6-NTRK3 fusion oncogene initiates breast cancer from committed mammary progenitors via activation of AP1 complex. *Cancer Cell*. 2007;12:542-558.
2. R. C. Rickert, J. Roes and K. Rajewsky: B lymphocyte-specific, Cre-mediated mutagenesis in mice. *Nucleic Acids Res*. 1997;25:1317-1318.
3. M. L. Churchman, J. Low, C. Qu, et al.: Efficacy of Retinoids in IKZF1-Mutated BCR-ABL1 Acute Lymphoblastic Leukemia. *Cancer Cell*. 2015;28:343-356.
4. J. Dang, L. Wei, J. de Ridder, et al.: PAX5 is a tumor suppressor in mouse mutagenesis models of acute lymphoblastic leukemia. *Blood*. 2015;125:3609-3617.
5. H. Li and R. Durbin: Fast and accurate short read alignment with Burrows-Wheeler transform. *Bioinformatics*. 2009;25:1754-1760.
6. A. Dobin, C. A. Davis, F. Schlesinger, et al.: STAR: ultrafast universal RNA-seq aligner. *Bioinformatics*. 2013;29:15-21.
7. S. Anders, P. T. Pyl and W. Huber: HTSeq--a Python framework to work with high-throughput sequencing data. *Bioinformatics*. 2015;31:166-169.
8. C. W. Law, Y. Chen, W. Shi, et al.: voom: Precision weights unlock linear model analysis tools for RNA-seq read counts. *Genome Biol*. 2014;15:R29.
9. E. C. Larsen, M. Devidas, S. Chen, et al.: Dexamethasone and High-Dose Methotrexate Improve Outcome for Children and Young Adults With High-Risk B-Acute Lymphoblastic Leukemia: A Report From Children's Oncology Group Study AALL0232. *J Clin Oncol*. 2016;34:2380-2388.
10. K. G. Roberts, Y. Li, D. Payne-Turner, et al.: Targetable kinase-activating lesions in Ph-like acute lymphoblastic leukemia. *N Engl J Med*. 2014;371:1005-1015.
11. N. Boulos, H. L. Mulder, C. R. Calabrese, et al.: Chemotherapeutic agents circumvent emergence of dasatinib-resistant BCR-ABL kinase mutations in a precise mouse model of Philadelphia chromosome-positive acute lymphoblastic leukemia. *Blood*. 2011;117:3585-3595.